ELSEVIER

Chemosphere 66 (2007) 1758–1764

CHEMOSPHERE

www.elsevier.com/locate/chemosphere

Role of biological activity and biomass distribution in air biofilter performance

Daekeun Kim, George A. Sorial *

Department of Civil and Environmental Engineering, University of Cincinnati, 765G Baldwin Hall, Cincinnati, OH 45221-0071, United States

Received 28 February 2006; received in revised form 26 June 2006; accepted 27 June 2006
Available online 7 August 2006

Abstract

The effects of temporal and spatial changes in biological activity and biomass amount on biofilter performance were investigated in a lab-scale trickle-bed air biofilter at a toluene loading of 46.9 g m^{-3} h^{-1} under two different experimental strategies, namely, periodic backwashing at a rate of 1 h once a week and 2 d starvation. Analysis of the overall reaction for toluene metabolism revealed that cell synthesis was relatively favored over toluene oxidation in the inlet section of the biofilter, but over time its oxidation became favored throughout the biofilter bed. Periodic in situ backwashing with media fluidization effectively made even spatial distribution of biomass along the bed media, by which consistent high removal performance in the biofilter has been attained. After 2 d starvation, the ratio of the biofilm EPS to the total biomass increased along the media bed depth, while the total biomass in the media bed subsequently decreased. The presence of sufficient biomass and microbial activity favorably influenced biofilter reacclimation after restart-up following starvation.

Keywords: Biodegradation; Biofilter; Biofiltration; Biomass; EPS; Microbial activity

1. Introduction

Biological degradation has been used extensively for controlling many kinds of contaminants. The effort in our research towards biological treatment has focused on biofiltration technology for volatile organic compound (VOC) removal from waste air streams. Our biofiltration research has expanded the range of application of biofiltration technology to the treatment of VOC under adverse operating conditions (i.e., non-use periods and fluctuating contaminant concentration). Different single chemicals were studied by our group (Cai et al., 2004, 2005; Kim et al., 2005a,b) to evaluate biofilter performance for long-term operation. Two significant findings were made. First, coordinated biomass control, i.e., periodic in situ backwashing with media fluidization, was effective in shearing off excess biomass from the packing media, thus inducing consistent high removal efficiencies in the biofilter. Recovery of removal efficiency in the biofilter after biomass control was a critical factor for evaluating the biofilter performance. Second, reacclimation of the biofilter to reach the 99% removal efficiency after non-use periods (i.e., starvation) was apparently different from that after backwashing, suggesting that the biofilter response after restart-up following non-use periods was dependent on the biomass retained in the media bed.

The amount of biomass can reflect the biofilter performance that is relevant to microbial activity (Devinny et al., 1996). Active microorganisms could be found in the biofilter where biomass accumulates rapidly. Excess accumulation of biomass causes severe biofilter operating problems including an increase in airflow resistance within the bed and low contaminant removal efficiencies (Smith et al., 1996; Weber and Hartmans, 1996; Iliuta and Larachi, 2004). Thus, coordinated biomass control is deemed necessary for achieving long-term performance of

* Corresponding author. Tel.: +1 513 556 2987; fax: +1 513 5562599.
E-mail address: George.sorial@uc.edu (G.A. Sorial).

0045-6535/$ - see front matter © 2006 Elsevier Ltd. All rights reserved.
doi:10.1016/j.chemosphere.2006.06.069

the biofilter. However, subsequent loss of active biomass following biomass control was found to lead to a temporary decrease in biofilter performance (Delhomenie et al., 2003; Kim et al., 2005b). Hence further investigation of biomass activity and accumulation is required to better assess and predict the long-term efficacy of biomass control methods.

In liquid phase bioreactors, starvation leads to changes in cells numbers, community composition, and physiological state (Konopka et al., 2002). Some studies (Zhang and Bishop, 2003; Lobos et al., 2005) reported that during starvation in a liquid phase bioreactor, the cells can consume easily biodegradable extracellular polymeric substances (EPS) in order to satisfy their requirements for maintenance energy and also could produce new EPS. A few studies reported the effect of starvation on biological activity and biomass variation in gas phase bioreactors (Martin and Loehr, 1996; Metris et al., 2001; Cox and Deshusses, 2002). Cox and Deshusses (2002) observed that 10–50% of biomass in the biofilter was lost during 7 d of starvation. During a period of starvation, the rate of endogenous respiration was found to decrease exponentially (Metris et al., 2001). After starvation, reacclimation time to original biofilter performance was shown to be hours to days according to the duration of starvation and the presence of alternative carbon source (Martin and Loehr, 1996). Since biofilter performance is affected by any changes in biological activity associated with biomass retention during starvation, further detailed investigations provide clear understandings of biological activity and biomass variation in gas phase bioreactors during a starvation condition.

This paper presents the results of investigations on the role of biological activity and biomass distribution in air biofilter performance when periodic in situ backwashing with media fluidization was employed as the biomass control strategy, and when the biofilter was exposed to periods of non-use, i.e., starvation without substrate loading. For this purpose, temporal and spatial changes in biomass activity and accumulation were explored using a trickle-bed air biofilter (TBAB) subjected to toluene removal.

2. Materials and methods

2.1. Lab-scale biofilter system

Laboratory studies employed a TBAB, which was constructed of seven cylindrical glass sections (Ace Glass Inc., Vineland, NJ) with an internal diameter of 76 mm and total length of 130 cm providing a total volume of 0.00589 m^3. A head space section in the top section was designed for VOC-containing air inlet and for housing the nutrient spray nozzle, while a bottom space at a bottom section was designed for the outlet of treated air and leachate. Each space has sampling ports to allow sampling of stream entering and leaving the biofilter, as well as axially along the medium bed four gas-sampling port, which were located at 7.6, 23, 38, and 53 cm from the bottom of bed of the reactor. The biofilter has been maintained at a constant operating temperature of 20 °C in a constant temperature chamber. The biofilter was operated in a co-current gas and liquid downward flow mode.

The air supplied to the biofilter was purified with complete removal of water, oil, carbon dioxide, VOCs, and particles by Balston FTIR purge gas generator (Paker Hannifin Coporation, Tewksbury, MA). The air flow to the biofilter was set up at the rate of 2.22 l min^{-1}, regulated by a mass flow controller (MKS Model 247C four-channel read-out mass flow controller, Andover, Mass). The corresponding empty bed retention time (EBRT) was 1.23 min. Liquid VOC was injected via a syringe pump (Harvard Apparatus, model NP 70-2208, Holliston, MA) into the air stream where it vaporized, and entered the biofilter through the topmost side port of the column. The liquid flow to the biofilter was set up at the rate of 2.4 l d^{-1} of a buffered nutrient solution, regulated by a programmable controller (Danaher Controls, Eagle Signal Model MX 190, Gurnee, IN). The feed was intermittently sprayed as a fine mist onto the top of the medium bed through a spray nozzle (Corrigan Corporation, Northbrook, IL).

Pelletized media (Celite® 6 mm R-635 Bio-Catalyst Carrier; Celite Corp., Lompoc, CA) were chosen as filter material for their high porosity enough to hold significant amounts water and nutrients as described elsewhere (Kim et al., 2005b). The media bed depth (L_0) was about 60 cm. The buffered nutrient solution was deionized and activated carbon filtered water, which contained all necessary macronutrients, micronutrients, and buffer as described elsewhere (Sorial et al., 1998). A COD-to-nitrogen ratio of 50:1 and a nitrogen-to-phosphorous ratio of 4:1 were maintained for a given VOC loading. Nitrate (NO_3–N) was used as the sole sources of nutrient-nitrogen. pH in the buffered nutrient solution has been maintained between 7.5 and 8.0 by using $NaHCO_3$.

2.2. Biofilter operation

The biofilter continued to be operated without reconditioning the media used in a previous experimental run (Kim et al., 2005c). In order to maintain constant high removal efficiency, the biofilter received influent air with 250 ppmv toluene, corresponding to a loading of 46.9 g m^{-3} h^{-1}. This loading was found to yield constant high biofilter performance in our previous study (Kim et al., 2005a). A periodic in situ backwashing was considered as the biomass control strategy. Backwashing was conducted while the biofilter was offline by using 18 l of the buffered nutrient solution to induce full medium fluidization at about 50% bed expansion for a defined time period. The details of the backwashing were described elsewhere (Smith et al., 1996; Sorial et al., 1998; Kim et al., 2005b). The backwashing duration and frequency were set at 1 h once a week for a period of three weeks. In order to avoid significant reduction in media bed volume through media sampling for biomass analysis, the media

bed was replenished with fresh pellets during the operation of backwashing. No significant decrease in biofilter performance has been observed subsequent to the replenishment of the media.

After a period of three cycles of backwashing, the starvation strategy was coordinated without other strategies of biomass control such as backwashing. The starvation strategy involves the period without toluene loading, i.e., pure air with nutrient flow through the biofilter. The duration and frequency for starvation were 2 d per week for a period of two weeks.

2.3. Analytical methods

Gas phase samples were taken with gas-tight syringes through low-bleed and high-puncture-tolerance silicone gas chromatograph (GC) septa installed in the sampling ports. Samples for toluene and carbon dioxide were immediately analyzed by using GCs (HP 5890, Series II, Hewlett Packard, Palo Alto, CA) equipped with flame ionization detector and thermal conductivity detector, respectively.

Liquid phase measurements included influent and effluent concentrations of nitrate, dissolved total carbon (TC), dissolved inorganic carbon (IC), and volatile suspended solids (VSS). Nitrate concentration was determined by measuring UV absorption at 220 nm using a Shimadzu UVmini 1240 UV–Vis spectrophotometer (Shimadzu Corp., Tokyo, Japan). TC and IC contents of the aqueous samples were determined by using a Shimadzu TOC 5000 analyzer (Shimadzu Corp., Tokyo, Japan). The VSS analysis was carried out according to Standard Methods 2540G (APHA, 1998).

Biomass analysis was performed to determine spatial variations in volatile solids (VS) as total biomass, and total carbohydrates and proteins as the biofilm EPS. 7 (±1) g of bed media covered with biomass was carefully collected from each sampling port in the biofilter. VS was determined according to Standard Method 2540G (APHA, 1998). Total carbohydrate concentration was determined by phenol reaction described by Daniels et al. (1994). 0.5–1.0 g of each wet media sample was mixed with 1 ml ultrapure water in the reaction vial. The sample was mixed with phenol and sulfuric acid and allowed to cool. The absorbance at 488 nm was compared to a glucose standard curve to determine the mass of carbohydrates per dry media mass. Proteins concentration was determined using Coomassie® Plus Proteins Assay Reagent (#23236) (Pierce Biotechnology, Rockford, IL). 0.5–1.0 g of each wet media sample was mixed with 2 ml MilliQ water in the reaction vial. 2-ml of the reagent was added and the solution was sonicated for 10 min. The absorbance at 595 nm was compared to a bovine serum albumin standard curve to determine the mass of proteins per dry media mass. All analyses were duplicated in order to ensure reproducibility and representativeness of the filter bed for each specific section.

3. Results and discussion

3.1. Biofilter performance

Fig. 1a provides toluene loading and removal, CO_2 production, and biomass loss as equivalent carbon in mol m^{-3} h^{-1} as a function of sequential time following backwashing. Nitrogen utilization is also presented in Fig. 1a. CO_2 production was estimated as the net analysis of influent and effluent in the gas streams and liquid streams coupled with inorganic carbon. For liquid phase, CO_2 production was estimated from the difference of IC concentration between the influent and effluent liquid. Biomass loss was estimated as the VSS loss from the effluent liquid (excluding the backwashed liquid) by assuming that a typical cellular composition for a heterogeneous microorganism can be represented by $C_5H_7O_2N$. Fig. 1a clearly shows that the biofilter achieved constantly high removal performance. The average removal efficiency was 98 ± 2%. A slight increase in CO_2 production rate was observed during the initial days following backwashing, while nitrogen utilization rate decreased slightly (detailed analysis is provided in the next section – biological activity). Generally, it has been observed that the detachment rate

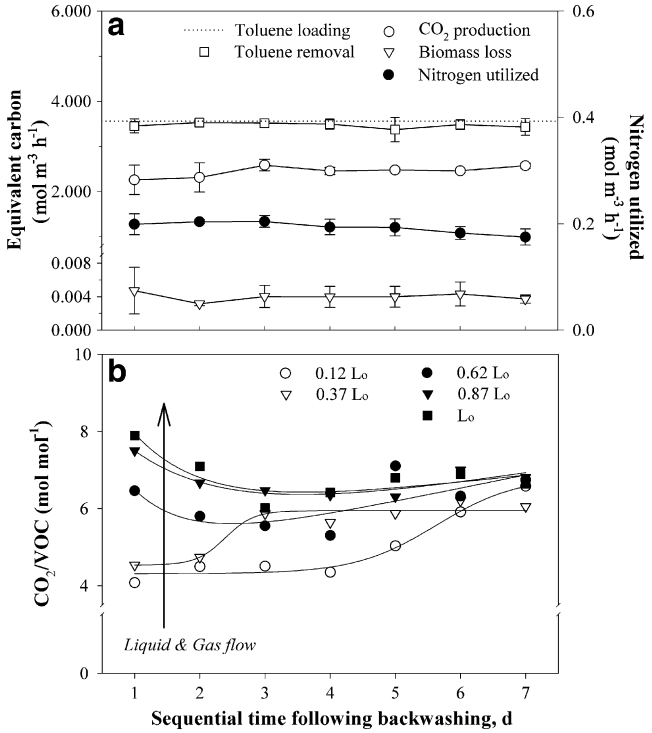

Fig. 1. Biofilter performance for three cycles of backwashing: (a) equivalent carbon and nitrogen utilized: The dotted line represents the corresponding toluene loading rate of 3.56 mol m^{-3} h^{-1} as carbon. The symbols represent the average experimental value and the error bars represent the standard deviation for three cycles of backwashing. (b) Molar ratio of CO_2 produced to toluene removed with bed media depth following backwashing: the symbols represent the average experimental value for three cycles of backwashing. The duration and frequency of backwashing was 1 h once a week. The bed media depth, $L_0 = 60$ cm.

of biomass increased with an increase in biomass accumulation (Trulear and Characklis, 1982), however, in our study no significant changes in biomass loss was observed (see Fig. 1). The total biomass washed out during the three times of backwashing amounted to 4.36 ± 0.83 g VSS, which accounted for 13% of the net carbon of the toluene consumed as seen in Table 1.

Assuming that the 38% unaccounted nitrogen reported in Table 1 was due to nitrate utilization as electron acceptor for energy production in addition to oxygen, denitrification would be responsible for excess nitrate utilization. It has been reported that denitrification activity was able to be present in the degradation of significant portion of organic carbon in an aerobic biofilter (du Plessis et al., 1998; Zhu et al., 1998). As the biomass retained within the system increased, it is speculated that denitrifying environment would develop due to deeper biofilm formation.

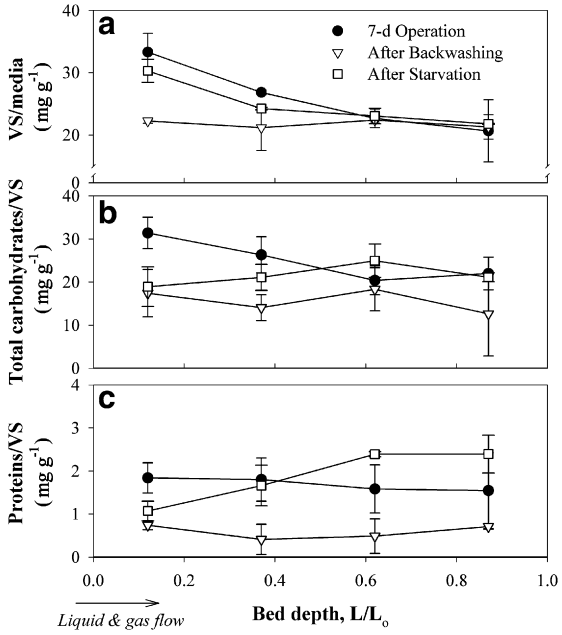

Fig. 2. Biomass distribution as a function of the media depth: (a) Volatile solids as total biomass; (b) total carbohydrates; (c) proteins. The symbols represent the average experimental value and the error bars represent the standard deviation for the different cycles of each experimental strategy. The bed media depth, $L_0 = 60$ cm.

3.2. Biological activity

The biofiltration has its most widespread use as a means to remove biodegradable electron donors from the waste gas stream. Microorganisms use an electron donor substrate for two principal processes, namely, cell synthesis and energy production (Rittmann and McCarty, 2001). The biological activity could be, thus, due to cell synthesis and energy production. The overall reaction for aerobic biodegradation of toluene under steady state condition is determined by the following half reaction (R_a, electron acceptor half reaction; R_c, cell synthesis half reaction; R_d, donor half-reaction):

$$R_a: 1/4O_2 + H^+ + e^- \rightarrow 1/2H_2O \quad (1)$$

$$R_c: 1/28NO_3^- + 5/28CO_2 + 29/28H^+ + e^- \rightarrow 1/28C_5H_7O_2N + 11/28H_2O \quad (2)$$

$$R_d(\text{written as oxidation}): 1/36C_7H_8 + 14/36H_2O \rightarrow 7/36CO_2 + H^+ + e^- \quad (3)$$

Since the faction of electrons used for energy generation (f_e) and synthesis (f_s) must equal 1.0 ($f_e + f_s = 1$), the overall reaction (R) becomes

$$R = f_eR_a + f_sR_c - R_d \quad (4)$$

$$C_7H_8 + 9f_eO_2 + 36/28f_sNO_3^- + 36(f_e + 29/28f_s - 1)H^+ \rightarrow 36/28f_sC_5H_7O_2N + (18f_e + 99/7f_s - 14)H_2O + (7 - 45/7f_s)CO_2 \quad (5)$$

A mass balance check provided in Table 1 shows that for aerobic biodegradation of toluene, 72% of the carbon equivalent in toluene removal was used for CO_2 production. Hence, based on Eq. (5), $f_s = 0.30$ and $f_e = 0.70$. The overall reaction for aerobic biodegradation of toluene at an organic loading rate of 46.9 g m^{-3} h^{-1} under steady state condition without accumulation of intermediate products and with nitrate used as nitrogen source is thus given by

$$C_7H_8 + 6.29O_2 + 0.39NO_3^- + 0.39H^+ \rightarrow 0.39C_5H_7O_2N + 2.84H_2O + 5.06CO_2 \quad (6)$$

Eq. (6) provides the general overall biodegradation reaction for toluene if no denitrification is taking place. Since biological activity varies along the biofilter depth and with

Table 1
Carbon recovery[a] and nitrogen recovery[b] during the experimental run with media backwashing

Carbon recovery, %					Nitrogen recovery, %		
[a]C_{CO_2}	[b]C_{VSS}	[c]C_{TOC}	[d]$C_{Backwashing}$	$C_{Unaccounted}$	[e]N	[f]N[c]	$N_{unaccounted}$
72	<1	2	13	12	47	15	38

[a] Carbon recovery: $C_{VOC\ removed} = {}^aC_{CO_2\ in\ effluent\ gas\ and\ effluent\ liquid} + {}^bC_{VSS\ in\ effluent\ liquid} + {}^cC_{Total\ organic\ carbon\ in\ effluent\ liquid} + {}^dC_{VSS\ washed\ out\ through\ backwashing} + C_{Biomass\ retained\ in\ the\ reactor}$. A typical cellular composition for a heterogeneous microorganism can be represented as $C_5H_7O_2N$.

[b] Nitrogen recovery: $N_{Nitrogen\ utilized} = N_{nitrogen\ used\ for\ biomass\ growth} + {}^eN_{nitrogen\ serve\ as\ electron\ acceptor}$. Since the net accumulation of attached biomass in the reactor is not equal to be zero, $N_{nitrogen\ used\ for\ biomass\ growth} = N_{VSS\ in\ effluent\ liquid\ and\ VSS\ washed\ out\ through\ backwashing} + {}^fN_{Biomass\ retained\ in\ the\ reactor}$.

[c] Estimated from $C_{unaccounted}$ in an assumption that the carbon unaccounted in the experiment results from the carbon retained in the reactor.

sequential date of operation, our finding for biological activity based on the overall reaction as represented by Eq. (6) is inevitably questioned.

In order to evaluate the temporal and spatial changes in biological activity along the biofilter, the microbial yield from substrate utilization is used in terms of the ratio of CO_2/VOC. CO_2 production was compared with toluene removal at different bed media depth as a function of sequential time following backwashing (see Fig. 1b). At the top portion of bed media (above $0.12L_0$), the molar ratio of CO_2 to toluene removed was initially 4.1 and then it increased with sequential time. The ratios also increased along the bed media. At the lower portions of the bed media ($0.62L_0$ and above), the ratio decreased with the sequential time. Finally, the molar ratios of CO_2 production to toluene removed along the biofilter depth approached a similar value with sequential time. It is worthwhile noting that limitation of nutrient and oxygen could develop along the bed depth. However, since sufficient nutrient were supplied and excess nitrate was measured in the effluent liquid, nutrients limitation could be negligible. Oxygen limitation generally depends on the VOC concentration and other factors such as medium types and biofilm structure (Zhu et al., 2004). As discussed by Smith et al. (2002), oxygen limitation begins to be a problem beyond an inlet concentration of 593 ppmv for toluene at 32 °C, indicating that oxygen limitation was not a problem in this study. It is, therefore, speculated from Fig. 1b that cell synthesis was relatively favored over toluene oxidation in the upper section of the biofilter. However, after a certain period when biomass grew sufficiently, toluene oxidation process predominated in the whole bed. As observed by Song and Kinney (2000), cell synthesis would be initially preferred in the inlet section of the biofilter. One possible explanation for this speculation is that less cell synthesis was involved in the lower section of the biofilter due to substrate limitation. During the experimental runs, more than 60% of the inlet toluene was degraded within the upper sections (above $0.37L_0$) while the lowest section (beyond $0.87L_0$) of the media contributed only to 0.05% of toluene removal. As discussed by Hwang and Tang (1997), local biological growth rate would be lower in the lower section of the biofilter due to low substrate concentration. Cherry and Thompson (1997) observed that without nutrient limitation, biomass subsequently grew until the substrate was used up, while biomass growth ceased in case of substrate limitation. Note that the qualitative composition of the biomass in different sections of the biofilter will impact the biological activity at various depths of the biofilter.

3.3. Biomass distribution

The profiles obtained for total biomass and biofilm EPS components, showing the concentrations of VS, total carbohydrates, and proteins as a function of the depth of bed media in the biofilter, are provided in Fig. 2. These profiles are provided for the two experimental strategies (backwashing and starvation) and are compared to those after 7-d operation. The profile after 7-d operation was obtained just prior to backwashing and starvation.

It is seen from Fig. 2a that a decrease in the amount of total biomass along the bed media was noticed after 7-d operation, i.e., less biomass grew in the bottom section of the biofilter. This behavior confirms our previous speculation that the synthesis process was relatively favored over the chemical oxidation in upper section of the biofilter. A concentration decrease of biofilm EPS in VS along the bed media was also noticed after 7-d operation as seen in Fig. 2b and c. The total carbohydrate/VS changed from $31.4 \pm 3.6\ mg\ g^{-1}$ to $21.9 \pm 3.8\ mg\ g^{-1}$, and proteins/VS changed from $1.8 \pm 0.4\ mg\ g^{-1}$ to $1.5 \pm 0.9\ mg\ g^{-1}$. It is speculated that EPS production is higher in the upper section of the biofilter where higher levels of electron donors are available in comparison to the subsections due to high microbial viability. In contrast to the observation after 7-d operation, backwashing of bed media achieved an even distribution of the EPS components as well as total biomass. These results support the findings in our previous studies (Smith et al., 1996; Sorial et al., 1998; Kim et al., 2005b), which indicated that periodic backwashing with media fluidization was very effective in preventing accumulation of excess biomass.

It is also seen from Fig. 2a that 2-d starvation provided a spatial decrease in total biomass compared to the 7-d operation. As discussed by Cox and Deshusses (2002), the decrease in biomass subjected to starvation would result from biomass death and lysis, endogenous respiration of microbial cultures in the system, predation by higher organisms, and shear by the liquid flow or gas flow. It is interesting to note that after starvation (see Fig. 2b and c), the ratio of EPS components to total biomass increased along the depth of bed media. In the lower section, the ratios after starvation were greater than those after 7-d operation. One possible explanation is that the release of lysis products made soluble EPS components increase along the bed media. In a study of the activated sludge in a membrane bioreactor (Lobos et al., 2005), an increase in soluble proteins concentration was observed during the starvation phase. Zhang and Bishop (2003) observed that the cells produced new EPS and gradually consumed the newly produced EPS during a starved state. They also found that the rate of EPS carbohydrates utilization were much faster than that of EPS proteins during EPS biodegradation. From this point of view, an increasing tendency of EPS proteins along media bed depth was much larger than that of EPS carbohydrates when the biofilter was exposed to a starved state. Overall, the starved state was subsequently attributed to a decrease in biomass within media bed, which could indicate that starvation can be considered as another means of biomass control. In our previous study (Kim et al., 2005a), stable 99% removal performance was observed for periodic starvation strategy (2 d of starvation for a week) for toluene loadings up to

18.8 g m^{-3} h^{-1} demonstrating that starvation can be practically utilized as biomass control at low loading rate where the biofilter does not potentially encounter clogging problem due to accumulation of excess biomass.

3.4. CO_2 production during starvation

During starvation, CO_2 evolution as an estimate of volumetric biological activity was explored (see Fig. 3). In Fig. 3a, the net CO_2 production rate (P_0) was plotted as a function of the sequential time of starvation. Fig. 3a indicates that the net CO_2 evolution significantly decreased during the first 2 h after shut down of toluene loading. A gradual decrease is noticed thereafter. This indicates that during starvation, the mixed cultures experienced endogenous respiration and the microbial activity slowly decreased. It is speculated that initially, easy biodegradable EPS was rapidly consumed and then microorganisms steadily lost their activity. The other possible explanation is that toluene adsorbed in the biomass itself might be first consumed and then biodegradable EPS was gradually consumed.

Fig. 3b shows the corresponding contribution to CO_2 production along the bed media. The percent CO_2 produced at a specific bed media depth is defined by the following equation:

$$\%CO_2 \text{ produced}_{i+1} = \frac{P_{i+1} - P_i}{P_0} \times 100 \quad (7)$$

where, P_i, net carbon production rate at a sampling port (i) along bed media; P_{i+1}, net carbon production rate at a sampling port ($i+1$) along bed media; P_0, net carbon production rate in effluent gas.

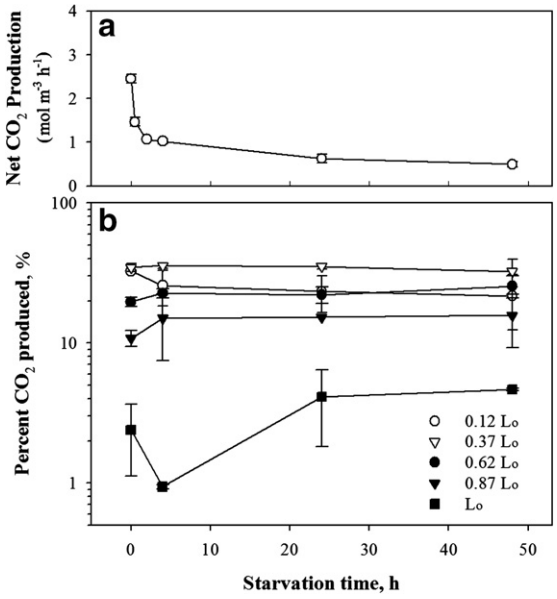

Fig. 3. CO_2 production during starvation period: (a) Effluent CO_2; (b) percent contribution to CO_2 production along the media depth. Gas and liquid flows were downward through the media. The bed media depth, $L_0 = 60$ cm. The symbols represent the average experimental value and the error bars represent the relative error for two cycles of starvation.

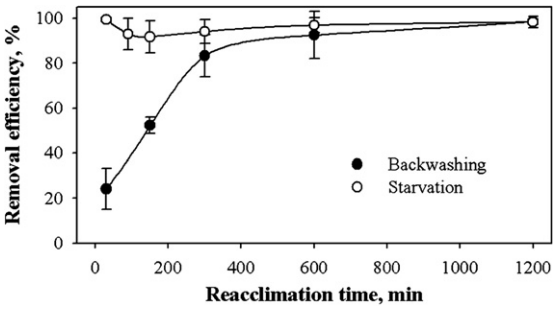

Fig. 4. Biofilter response after the restart-up following backwashing and starvation: The symbols represent the average experimental value and the error bars represent the standard deviation for the different cycles of each experimental strategy. Data presented is reproduced from Kim et al. (2005a).

Initially, 33% of the total CO_2 produced was detected up to $0.12L_0$ of the bed media. The contribution in the top portion gradually decreased to approximately 22% in 48 h. Relatively, constant contribution was observed at a bed depth of $0.37L_0$. In the case of the lower section of the biofilter (>0.37 L_0), the contribution gradually increased from approximately 33% to 47%. This behavior correlates with the increase in EPS components along the bed media during starvation (see Fig. 2). We speculate that higher CO_2 production evolved from endogenous respiration. It is interesting to note that during 2-d starvation, the microbial activity was not totally exhausted. This observation subsequently influenced the biofilter reacclimation to the original performance. As seen in Fig. 4, the response after substrate starvation was significantly different from that after backwashing. In case of starvation, the biomass retained in the system played a significant role in high removal efficiency of the substrate. This behavior would be due to initial adsorption of toluene on biomass. After that, vigorous microbial activity attributed to the biofilter recovery to high removal performance as compared to backwashing. The biofilter response after restart-up following starvation was not only affected by the amount of biomass and EPS materials, but also by the microbial activity that remained in the system.

Acknowledgements

This research was supported by National Science Foundation under award # BES 0229135. The finding and conclusions expressed in this publication are solely those of the authors and do not necessary reflect the views of the Foundation.

References

APHA, 1998. Standard Methods for the Examination of Water and Wastewater. American Public Health Association/American Water Works Association/Water Pollution Control Federation, Washington, DC.

Cai, Z., Kim, D., Sorial, G.A., 2004. Evaluation of trickle-bed air biofilter performance for MEK removal. J. Hazard. Mater. 114, 153–158.

Cai, Z., Kim, D., Sorial, G.A., 2005. Removal of methyl isobutyl ketone from contaminated air by trickle-bed air biofilter. J. Environ. Eng.—ASCE 131, 1322–1329.

Cherry, R.S., Thompson, D.N., 1997. Shift from growth to nutrient-limited maintenance kinetics during biofilter acclimation. Biotechnol. Bioeng. 56, 330–339.

Cox, H.H.J., Deshusses, M.A., 2002. Effect of starvation on the performance and re-acclimation of biotrickling filters for air pollution control. Environ. Sci. Technol. 36, 3069–3073.

Daniels, L., Hanson, R.S., Phillips, J.A., 1994. Chemical analysis. In: Gerhardt, P. (Ed.), Methods for General and Molecular Bacteriology. American Society for Microbiology, Washington, DC.

Delhomenie, M.C., Bibeau, L., Gendron, J., Brzezinski, R., Heitz, M., 2003. A study of clogging in a biofilter treating toluene vapors. Chem. Eng. J. 94, 211–222.

Devinny, J.S., Deshusses, M.A., Webster, T.S., 1996. Biofiltration for Air Pollution Control. Lewis Publishers, Boca Raton, FL.

du Plessis, C.A., Kinney, K.A., Schroeder, E.D., Chang, D.P.Y., Scow, K.M., 1998. Denitrification and nitric oxide reduction in an aerobic toluene-treating biofilter. Biotechnol. Bioeng. 58, 408–415.

Hwang, S.J., Tang, H.M., 1997. Kinetic behavior of the toluene biofiltration process. J. Air Waste Manage. 47, 664–673.

Iliuta, I., Larachi, F., 2004. Transient biofilter aerodynamics and clogging for VOC degradation. Chem. Eng. Sci. 59, 3293–3302.

Kim, D., Cai, Z., Sorial, G.A., 2005a. Behavior of trickle-bed air biofilter for toluene removal: effect of non-use periods. Environ. Prog. 24, 155–161.

Kim, D., Cai, Z., Sorial, G.A., 2005b. Evaluation of trickle-bed air biofilter performance under periodic stressed operating conditions as a function of styrene loading. J. Air Waste Manage. 55, 200–209.

Kim, D., Cai, Z., Sorial, G.A., 2005c. Impact of interchanging VOCs on the performance of trickle-bed air biofilter. Chem. Eng. J. 113, 153–160.

Konopka, A., Zakharova, T., Nakatsu, C., 2002. Effect of starvation length upon microbial activity in a biomass recycle reactor. J. Ind. Microbiol. Biotechnol. 29, 286–291.

Lobos, J., Wisniewski, C., Heran, M., Grasmick, A., 2005. Effects of starvation conditions on biomass behaviour for minimization of sludge production in membrane bioreactors. Water Sci. Technol. 51, 35–44.

Martin, F.J., Loehr, R.C., 1996. Effect of periods of non-use on biofilter performance. J. Air Waste Manage. 46, 539–546.

Metris, A., Gerrard, A.M., Cumming, R.H., Weigner, P., Paca, J., 2001. Modelling shock loadings and starvation in the biofiltration of toluene and xylene. J. Chem. Technol. Biotechnol. 76, 565–572.

Rittmann, B.E., McCarty, P.L., 2001. Environmental Biotechnology: Principles and Applications. McGraw-Hill, Boston.

Smith, F.L., Sorial, G.A., Suidan, M.T., Breen, A.W., Biswas, P., Brenner, R.C., 1996. Development of two biomass control strategies for extended, stable operation of highly efficient biofilters with high toluene loadings. Environ. Sci. Technol. 30, 1744–1751.

Smith, F.L., Sorial, G.A., Suidan, M.T., Biswas, P., Brenner, R.C., 2002. Development and demonstration of an explicit lumped-parameter biofilter model and design equation incorporating Monod kinetics. J. Air Waste Manage. 52, 208–219.

Song, J.H., Kinney, K.A., 2000. Effect of vapor-phase bioreactor operation on biomass accumulation, distribution, and activity: linking biofilm properties to bioreactor performance. Biotechnol. Bioeng. 68, 508–516.

Sorial, G.A., Smith, F.L., Suidan, M.T., Pandit, A., Biswas, P., Brenner, R.C., 1998. Evaluation of trickle-bed air biofilter performance for styrene removal. Water Res. 32, 1593–1603.

Trulear, M.G., Characklis, W.G., 1982. Dynamics of biofilm processes. J. Water Pollut. Con. F. 54, 1288–1301.

Weber, F.J., Hartmans, S., 1996. Prevention of clogging in a biological trickle-bed reactor removing toluene from contaminated air. Biotechnol. Bioeng. 50, 91–97.

Zhang, X.Q., Bishop, P.L., 2003. Biodegradability of biofilm extracellular polymeric substances. Chemosphere 50, 63–69.

Zhu, X.Q., Alonso, C., Suidan, M.T., Cao, H.W., Kim, B.J., Kim, B.R., 1998. The effect of liquid phase on VOC removal in trickle-bed biofilters. Water Sci. Technol. 38, 315–322.

Zhu, X.Q., Suidan, M.T., Pruden, A., Yang, C.P., Alonso, C., Kim, B.J., Kim, B.R., 2004. Effect of substrate Henry's constant on biofilter performance. J. Air Waste Manage. 54, 409–418.